

THEORETICAL AND NUMERICAL INVESTIGATION ON INTERNAL INSTABILITY PHENOMENA IN COMPOSITE MATERIALS

A. CARPINTERI, M. PAGGI AND G. ZAVARISE

Department of Structural and Geotechnical Engineering, Politecnico di Torino,
C.so Duca degli Abruzzi 24, 10129 Torino, Italy

ABSTRACT

Instability phenomena occurring in the microstructure of composite materials are investigated. To this aim, a complete description of the mechanical behavior of bi-material interfaces in composite materials requires the definition of both a cohesive law involving damage for the debonding stage, and a contact model during the closure of the interface. Both formulations are herein presented and implemented in the FE code FEAP. Numerical examples showing the transition from a snap-back instability to a stable mechanical response are presented.

1 INTRODUCTION

The mechanical behavior of advanced structures composed by different materials is strongly influenced by damage phenomena occurring at interfaces. These problems have a considerable importance in traditional fiber-reinforced composites, as well as in new-conception structural components.

In this paper, a fully comprehensive micromechanical approach for modeling the evolution of damage in metal matrix composites due to interfacial debonding between matrix and inclusions is proposed. Zero-thickness interfaces are modeled as special contact elements in which both the geometrical relationships intercurring between the nodes of the discretized problem, and the micromechanical constitutive laws are defined. Micromechanical cohesive and contact laws are then implemented in the FE code FEAP. According to damage mechanics, degradation of the cohesive properties due to cyclic loading is also accounted for, in order to study fatigue crack growth at bi-material interfaces. This innovative approach allows to model interface debonding and a subsequent closure of the debonded region in case of cyclic loading conditions.

Instability phenomena in the microstructure of composite materials are then investigated, paying special attention to size-scale transition from unstable to stable mechanical behaviors.

2 COHESIVE CONSTITUTIVE LAW

Linear elastic fracture mechanics has proven to be a useful tool for solving fracture problems, provided that a crack-like notch or flaw exists in the body and the nonlinear zone ahead of the crack tip is negligible. These conditions are not always fulfilled and, for both metallic and cementitious materials, among others, the size of the nonlinear zone due to plasticity or microcracking is not negligible with respect to other dimensions of the cracked geometry. The localized damaged material may be modeled as a pair of surfaces with no volume between them and its action can be replaced by an equivalent traction on the surfaces. Following Dugdale [1] and Barenblatt [2], this idea has been extensively applied to materials which are commonly classified as quasibrittle such as glassy, polymers, rocks, reinforced ceramics, concrete and composites. The *fictitious crack model* was pioneering introduced for concrete by Hillerborg et al. [3]. Then, Carpinteri, using for the first time the terminology *cohesive model*, applied this method to the study of ductile-brittle transition and snap-back instability in concrete [4,5]. A huge amount of

effort has been devoted to the implementation of the formulation into the finite element framework, mainly by Wawrzynek and Ingraffea [6] and by Carpinteri et al. [7], among others. More recently, a cohesive zone model for metal matrix composites (MMC) has been proposed by Tvergaard [8] and it is adopted in this paper since the behavior of MMCs is here investigated. In this formulation, a measure of the interface opening, λ , is given by

$$\lambda = \sqrt{\left(\frac{g_N}{l_{Nc}}\right)^2 + \left(\frac{g_T}{l_{Tc}}\right)^2}, \quad (1)$$

where g_N and g_T denote, respectively, the normal and the tangential separation. Parameters l_{Nc} and l_{Tc} represent the critical values for the normal and the tangential gap. They correspond to the separation for which cohesive forces transmitted through the interface vanish, i.e. a complete debonding takes place. Normal and tangential cohesive tractions are given as functions of interface opening in the process zone

$$\sigma_N = \frac{g_N}{l_{Nc}} P(\lambda), \quad \sigma_T = \gamma \frac{g_T}{l_{Tc}} P(\lambda), \quad (2)$$

where $P(\lambda)$ is defined as [8]:

$$P(\lambda) = \begin{cases} \frac{27}{4} \sigma_{\max,0} (1 - 2\lambda + \lambda^2) & \text{for } 0 \leq \lambda \leq 1, \\ 0 & \text{otherwise.} \end{cases} \quad (3)$$

In eqn (3) the parameter $\sigma_{\max,0}$ denotes the peak value of the normal cohesive traction before the softening branch. Moreover, $\gamma = \tau_{\max,0}/\sigma_{\max,0}$ represents the ratio between the peak values of normal and tangential tractions that can be separately specified in the model. For the sake of simplicity, in the sequel we consider $\gamma=1$, as already assumed in [8].

This cohesive formulation is herein extended by considering elastic unloading and reloading paths described by the following equations

$$\sigma_N = \frac{g_N}{l_{Nc}} P(\lambda_{\max}), \quad \sigma_T = \gamma \frac{g_T}{l_{Tc}} P(\lambda_{\max}), \quad (4)$$

where $P(\lambda_{\max})$ corresponds to $P(\lambda)$ computed at the maximum experienced interface separation during the previous loading history. As a result, unloading paths are linear and prescribed to occur to the origin of the traction-separation space. Reloading follows the same path up to the maximum interface separation λ_{\max} .

In addition to the above traction-separation relations, a description of the damage evolution has to be provided in order to capture finite life effects in the case of cyclic loading. To this aim, at each step, initial cohesive strengths $\sigma_{\max,0}$ and $\tau_{\max,0}$ are replaced by the actual cohesive strengths σ_{\max} and τ_{\max} which take into account the degradation of the cohesive law

$$\sigma_{\max} = \sigma_{\max,0}(1-D); \quad \tau_{\max} = \tau_{\max,0}(1-D), \quad (5)$$

where D is the damage variable, as introduced in [9].

To compute the current state of damage, a description of the evolution of damage has to be provided. For cyclic loading, the damage evolution equation has to characterize the failure of the cohesive model due to cyclic at subcritical loads. The fundamental hypotheses of the model are: (1) damage starts to accumulate when a deformation measure is greater than a critical value; (2) the increment of damage is related to the increment of deformation weighted by the current load level; (3) an endurance limit, i.e. a stress below which cyclic can proceed infinitely without failure, exists. According to these hypotheses, the increment of damage at time t is given by

$$\dot{D} = \frac{\Lambda^t - \Lambda^{t-\Delta t}}{\lambda_{\max}} \left[\frac{|\sigma|}{\sigma_{\max}} - \frac{\sigma_{th}}{\sigma_{\max,0}} \right] H(\Lambda^t - \lambda_0) \quad 0 \leq \dot{D} \leq 1, \quad (6)$$

where λ_{\max} represents the maximum non-dimensional cumulative separation length to get the failure of the cohesive zone; σ_{th} is a stress threshold value under which no damage occurs; H designates the Heaviside function; and λ_0 denotes the value of the cohesive separation corresponding to the peak strength σ_{\max} . The remaining parameters are the resultant traction, $|\sigma|$, and the cumulated interface separations computed at times t and $t-\Delta t$

$$\begin{aligned} |\sigma| &= \sqrt{\sigma_N^2 + \sigma_T^2}, \\ \Lambda^t &= \sum_{\substack{0 \rightarrow t \\ \Delta\lambda > 0}} \Delta\lambda. \end{aligned} \quad (7)$$

It is important to notice that the summation in eqn (7) of the separation increments is extended to positive increments only. In practice, this implies that reloading contributes to damage accumulation, whereas unloading does not. The current damage is computed as

$$D = \int \dot{D} dt. \quad (8)$$

3 MICROMECHANICAL CONTACT MODEL

A simulation of fatigue crack growth at bi-material interfaces for problems characterized by tension-compression cyclic loading requires not only the description of the interface debonding behavior, but also a proper modeling of the crack closure. The main problem underlying the use of a simple penalty method is given by the fact that it is difficult to choose the value of the penalty parameter consistent with the description of the real phenomenon. A more sophisticated and efficient approach can be adopted by defining a contact stiffness based on microscopical contact models. Such micromechanical laws are strongly nonlinear and are usually based on either statistical or fractal descriptions of the rough disbonded interface. Images obtained with the scanning electron microscope (SEM) can be then profitably used for the evaluation of contact parameters. A detailed review of some of the most important contact models can be found in [10]. In this paper, the fractal formulation by Majumdar and Bhushan [11] is adopted. Description of the implementation of this microscopical contact model in the FE framework is reported in [12].

4 SETUP FOR FEM COMPUTATIONS

Interfaces are modeled as contact surfaces and special contact elements. Both the geometrical relationships intercurring between the nodes of the discretized problem, and the constitutive laws are introduced in the proposed formulation. Depending on the contact status, an automatic switching procedure is adopted in order to choose between cohesive and micromechanical contact laws.

Furthermore, in order to decouple the discretization of the interface from that of the continuum, the virtual node technique is adopted, hence an arbitrary number of gauss points can be placed inside each contact element. The contribution of cohesive and contact forces can be explicitly added to the global virtual work equation

$$\delta W = \bigcup (F_N \delta g_N + F_T \delta g_T). \quad (9)$$

The proposed approach should be used to solve problems where high precision is required. Therefore an implicit strategy is adopted and the linearization of the equation set (9) is performed

$$\Delta\delta W_d = \left(\frac{\partial F_N}{\partial g_N} \Delta g_N + \frac{\partial F_N}{\partial g_T} \Delta g_T \right) \delta g_N + \left(\frac{\partial F_T}{\partial g_N} \Delta g_N + \frac{\partial F_T}{\partial g_T} \Delta g_T \right) \delta g_T + F_N \Delta \delta g_N + F_T \Delta \delta g_T, \quad (10)$$

where symbols δ and Δ denote, respectively, variations and linearizations. In eqn set (10) normal and tangential tractions are given by either the cohesive formulation or the contact model.

5 INSTABILITY PHENOMENA AND SIZE-SCALE EFFECT

The problem of debonding between matrix and inclusions in a representative cell of a metal-matrix composite is investigated. Mechanical and geometrical parameters are chosen to represent an aluminium alloy 2124-SiC whisker-reinforced material, as reported in [8]. In order to study the effect of the nonlinear behavior of the interface on the mechanical response, materials are assumed to be linear elastic. The horizontal macroscopic stress, σ_1 , normalized to the aluminium yield stress, σ_y , versus the applied mean strain is depicted in Fig. 1b.

In the case of monotonic horizontal displacement loading, the homogenized mechanical response is given by the curve A in Fig.1b. It is important to notice that a significant reduction in stiffness occurs when ε_l exceeds 0.04. At that point, a sudden debonding of some elements along the interface takes place, suggesting the occurrence of snap-back instability. This phenomenon was also observed by Piva and Viola [13] using an analytical approach. From the numerical point of view, a crack-length control scheme should be adopted [4] to follow the dashed part of the snap-back curve.

Following Carpinteri [5], in order to predict the transition from snap-back instability to a stable mechanical response, a Dimensional Analysis and the Buckingham's Π Theorem can be applied in order to define the dimensionally independent quantities whose variations characterize the macroscopic behavior

$$F = \Pi \left(\sigma_y, b, G_{ic}^i, \Delta u, \frac{\sigma_{\max,0}}{\sigma_y}, \frac{E_f}{E_m}, \frac{V_f}{V_f + V_m}, \nu_f, \nu_m \right), \quad (11)$$

$$\frac{\sigma_1}{\sigma_y} = \Pi \left(\frac{G_{ic}^i}{\sigma_y b}, \varepsilon_1, \frac{\sigma_{\max,0}}{\sigma_y}, \frac{E_f}{E_m}, \frac{V_f}{V_f + V_m}, \nu_f, \nu_m \right),$$

where parameters F , σ_y , b , G_{ic}^i and Δu denote, respectively, the resultant horizontal load, the matrix yield stress, the size of the representative cell, the interface fracture energy and the imposed horizontal displacement. Parameters E_f , E_m , ν_f , ν_m in eqn (11) represent the elastic moduli and the Poisson's ratios of the inclusion and the matrix, whereas the ratio $V_f/(V_f + V_m)$ is the inclusion volumetric fraction.

According to Carpinteri [5], a scale interaction between plastic collapse and brittle fracture in concrete composites is ruled by the brittleness number $s_E = G_{ic}^i / \sigma_y b$. For a reinforcement volumetric fraction equal to 0.46 and by assuming scale-invariant mechanical parameters, it is possible to investigate the mechanical response by varying the size of the cell b . As a consequence, the inclusion diameter scales as b and higher values of the brittleness number correspond to a finer grained material. By considering four values of the cell size corresponding to $b = 2.6 \mu\text{m}$, $5.2 \mu\text{m}$, $6.8 \mu\text{m}$ and $10.4 \mu\text{m}$, the corresponding brittleness numbers and the resulting mechanical behaviors are shown in Fig.1b (curves A, B, C and D). It is important to notice that the snap-back instability disappears by reducing the size of the inclusion and the transition from snap-back to a stable softening branch occurs for particles whose diameter is approximately equal to $5.2 \mu\text{m}$. In general, the critical cell size depends both on the mechanical properties of the constituent materials, and on the inclusion volumetric fraction.

The mechanical behavior of the one-inclusion problem subjected to a horizontal tension-compression cyclic loading is also investigated and macroscopic results are depicted in Fig.1c (curve B). During the first cycle the macroscopic response corresponds to a perfectly bonded configuration whose elastic modulus can be estimated according to mixture rules.

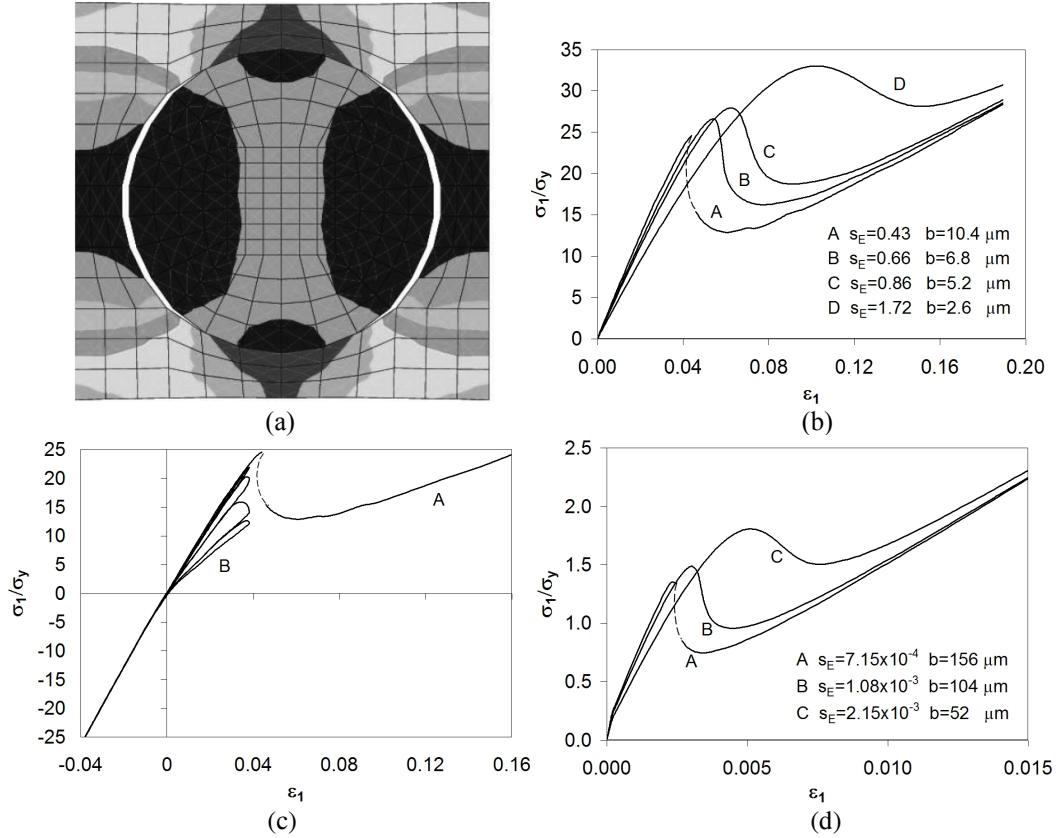


Figure 1: One-inclusion problem: (a) mesh; (b) non-dimensional horizontal macroscopic stress vs. horizontal deformation for composites characterized by different brittleness numbers; (c) non-dimensional horizontal macroscopic stress vs. horizontal deformation for (A) monotonic and (B) cyclic displacement loading; (d) realistic macroscopic response.

In the sequel, since damage increases cycle by cycle, a progressive reduction in stiffness occurs. For these problems, the numerical approach herein presented permits to obtain an estimation of the effective elastic modulus which cannot be provided by simplified mixture rules. Numerical results obtained consistently to input data in [8] are characterized by particularly high values of the horizontal stress. More realistic results in agreement with the value of the aluminium yield stress can be obtained by considering the cohesive peak stress equal to the matrix yield stress, i.e. $\sigma_{\max,0}=\sigma_y$ (see Fig.1d). Also in this case, a transition from unstable to stable behaviors can be obtained by reducing the size of the inclusion.

6 CONCLUSIONS

The numerical approach herein presented, starting from [12,14], constitutes a step forward in the modeling of interface problems in fibrous composite materials. From the mechanical point of view, a particular attention is devoted to the interface constitutive laws.

From the numerical viewpoint, interfaces are modeled as contact surfaces with the virtual node technique. Due to this approach, the discretization of the interface can be treated independently from that of the continuum and the study of large multiple-inclusion problems will be possible. According to the proposed method, internal instability phenomena in fiber-reinforced composites have been investigated and the Carpinteri's brittleness number has been profitably used for characterizing the size-scale transition from unstable to stable behaviors.

7 ACKNOWLEDGEMENTS

Support of the Italian Ministry of University and Scientific Research (MIUR) is gratefully acknowledged.

8 REFERENCES

- [1] Dugdale D.S.: Yielding in steel sheets containing slits, *J. Mech. Phys. Solids*, Vol. 8, pp. 100-104 (1960).
- [2] Barenblatt G.I.: The mathematical theory of equilibrium cracks in brittle fracture, in H.L. Dryden, T. Von Karman (Eds.), *Advances in Applied Mechanics*, Vol. VII, Academic Press, New York, pp. 55-129 (1962).
- [3] Hillerborg A., Modeer M., Petersson P.E.: Analysis of crack formation and crack growth in concrete by means of fracture mechanics and finite elements, *Cement and Concrete Res.*, Vol. 6, pp. 773-782 (1976).
- [4] Carpinteri A., Di Tommaso A., Fanelli M.: Influence of material parameters and geometry on cohesive crack propagation, in *Fracture Toughness and Fracture Energy of Concrete* (Proceedings of an International Conference on Fracture Mechanics of Concrete, Lausanne, Switzerland, 1985), Ed. F.H. Wittmann, Elsevier, Amsterdam, pp. 117-135 (1986).
- [5] Carpinteri A.: Cusp catastrophe interpretation of fracture instability, *J. Mech. Phys. Solids*, Vol. 37, pp. 567-582 (1989).
- [6] Wawrzynek P.A., Ingraffea A.R.: Interactive finite element analysis of fracture processes: an integrated approach, *Theor. Appl. Fract. Mech.*, Vol. 8, pp. 137-150 (1987).
- [7] Carpinteri A. (Ed.): *Nonlinear Crack Models for Nonmetallic Materials*, Dordrecht: Kluwer Academic Publisher (1999).
- [8] Tvergaard V.: Effect of fiber debonding in a whisker-reinforced metal, *Mat. Sci. Engng A*, Vol. 107, pp. 23-40 (1990).
- [9] Roe K.L., Siegmund T., An irreversible cohesive zone model for interface fatigue crack growth simulation, *Engng. Fract. Mech.*, Vol. 70, pp. 209-232 (2003).
- [10] Zavarise G., Borri-Brunetto M., Paggi M.: On the reliability of microscopical contact models, *Wear*, in press (2004).
- [11] Majumdar A., Bhushan B.: Fractal model of elastic-plastic contact between rough surfaces, *ASME J. Trib.*, Vol. 113, pp. 1-11 (1991).
- [12] Zavarise G., Borri-Brunetto M., Paggi M.: Prediction of real contact area for interfacial debonding damage in fibrous composite materials, *Proceedings of the 16th AIMETA Congress of Theoretical and Applied Mechanics*, Ferrara, Italy (2003).
- [13] Piva A., Viola: Fracture behaviour by two cracks around an elliptic rigid inclusion, *Engng. Fract. Mech.*, Vol. 15, pp. 303-325 (1981).
- [14] Wriggers P., Zavarise G., Zohdi T.I.: A computational study of interfacial debonding damage in fibrous composite materials, *Comp. Mat. Sci.*, Vol. 12, pp. 39-56 (1998).